Mode locking and sideband generation: A mechanism for intermediate stochasticity in conservative systems

Y. Gell and R. Nakach
Association Euratom Commissariat à l'Energie Atomique sur la Fusion Contrôlée, Centre d'Etudes Nucléaires Cadarache, 13108 St. Paul Lez Durance CEDEX, France
(Received 31 May 1989; revised manuscript received 30 May 1990)

We present a numerical study of the two-wave system that reveals the occurrence of stochasticity for a limited range of the perturbation only, beyond that it disappears. We refer to this type of stochasticity as "intermediate stochasticity." Using a Fourier analysis, it is found that intermediate stochasticity is closely associated with the mode-locking phenomenon taking place in the system. A theoretical analysis of this phenomenon, based on an extension of the Krylov-Bogoliubov theory of slow variation parameters, which is appropriate to strongly nonlinear equations, is presented. This analysis explains the main qualitative features of the numerical observations.

I. INTRODUCTION

The chaotic behavior of dynamical systems has been a major research subject in the physical sciences for the past 30 years and is still actively pursued. The impetus for this research was the formulation and proof of the celebrated Kolmogorov-Arnold-Moser[1] (KAM) theorem. This theorem is fundamentally concerned with Hamiltonian systems having a finite number of degrees of freedom, which are sufficiently closed to completely integrable ones. It establishes the conditions under which the stability of generalized surfaces or tori in phase space remains intact while increasing the strength of the perturbation in the system. Once these conditions have been violated, one can expect unorderly or chaotic motion to set in.

The practical phenomenological criterion for the breaking down of the KAM surfaces has been studied by Chirikov[2] and is expressed in terms of overlapping of neighboring nonlinear resonances. Refinements of this criterion have been proposed by different authors, an account of which can be found in Ref. 3. This criterion essentially claims that once the strength of the perturbation reaches a threshold for which two neighboring resonances do overlap, stochasticity is insured and increasing the perturbation further will generally make the motion even more chaotic. However, one can encounter situations for which this basic scheme for arriving at stochasticity is not followed. Indeed, even in a Hamiltonian system as simple as the one describing the one-dimensional motion of a particle in two electrostatic waves, stochasticity might set in for a given value of the perturbation and may disappear suddenly when the perturbation parameter is further increased. Increasing this parameter still more, while all other parameters are kept fixed, leads to the reappearance of stochasticity for which further increase of the perturbation parameter will not stabilize the motion anymore. We refer to this intermediate stage in the evolution of the system arriving possibly to chaos as "intermediate stochasticity."

In Sec. II, we give a numerical study of the two-wave system presenting some examples corresponding to different sets of parameters and initial values for which such an intermediate stochasticity phenomenon is exhibited. This study consists of a dual complementary representation of the solution of the equation of motion. One representation utilizes the well-known Poincaré surface of section method in phase space, the other being the standard Fourier power spectrum analysis of the velocity of the particle under consideration. This last technique enables one to follow the dependency of each individual mode on the parameters of the system, thus allowing the detection of any peculiarity in this dependency. Inspecting the power spectrum, a striking feature was revealed: the locking of a specific mode to a characteristic frequency inherent to the system. This locking was found to persist with changes of the perturbation within a finite parameter range.

The analysis of the mode spectrum is conveniently done considering three different regimes of the perturbation parameter: (i) the perturbation parameter is below the mode-locking threshold; (ii) the mode is locked to the characteristic frequency; (iii) the perturbation parameter is increased until the mode becomes unlocked again. In this work we will be mainly concerned with the first regime. Detailed studies of the other two regimes will not be given here. Considering the first regime for which the modes are still unlocked, we find it instructive to look separately at the case in which the mode is well below the threshold of locking and to the case when it is close to this threshold. In the first case, there is a production of beat notes, between the characteristic mode and the mode under consideration, in the second case, the spacing between the beat notes might become very small, so that a strongly distorted beat note is generated. The generation of these slightly shifted beat notes, in conjunction with the nonlinear mixing effect resulting from the nonlinearity of the equation of motion, allows for the proliferation of low-frequency modes in the power spectrum resulting in its global raise. This is the signature of chaotic behav-

ior of the system. At this stage, a further increase of the perturbation may shift the frequency of the mode bringing it into its locking range, the effect of which is the extinction of the low-frequency modes that had been generated when the system was close to the threshold of locking. Consequently, a pattern of well-defined and separated peaks is reestablished in the spectrum, signifying a regular motion. This termination of the chaotic behavior of the motion with an increase of the perturbation is characterizing the intermediate stochasticity.

Having recognized the significance of the locking phenomenon in this stochastic mechanism, we proceed in Sec. III to analyze the conditions of its occurrence. This analysis utilizes a basic formalism we developed[9] that enables the prediction of synchronized oscillations for a given system. This formalism has as its point of departure the method of variation of parameters widely known as the perturbation theory of Krylov and Bogoliubov,[5] which is in fact a development of the earlier formalism of Van der Pol.[6] Considering values of the perturbation in a range close to the threshold of locking, we evaluate the shifting of the frequency of the relevant mode. As a result of this shifting, closely separated sidebands are found to be generated, leading to the existence of the above-mentioned low-frequency beat notes.

Now, due to the nonlinear cascading process taking place in the system,[7] these low-frequency beat notes combine with all the other modes, resulting in a diffused pattern of the power spectrum. We suggest this mechanism to be at the origin of the intermediate stochasticity.

II. NUMERICAL STUDY OF THE EQUATION OF MOTION

We consider the nonlinear two-wave differential equation. This equation describes a variety of physical processes and has the same generic form as the one describing the motion of a particle in a system consisting of two electrostatic waves propagating in the same direction and having different phase velocities. In its normalized form this equation reads

$$\frac{d^2x}{dt^2}+\sin x=-\epsilon\sin(\alpha x-\nu t)\ , \tag{1}$$

where ϵ is considered as a small parameter and α and ν are, respectively, the normalized wave number and frequency parameters of the perturbation. The initial position and velocity of the particle determine the nature of its motion whether it is confined or not within the separatrix in phase space (for a trapped or an untrapped particle). In a search for the route to chaos and for exhibiting the phenomenon of intermediate stochasticity, we limit ourselves, in the following, to motion corresponding to untrapped particles far away from the separatrix. Previous experience in analyzing such motions shows the effectiveness of using a dual representation of the solution of the equation consisting of a phase-space picture together with a complementary Fourier description. We thus undertook the numerical solution of Eq. (1) and use the well-known Poincaré surface of section method to visualize this motion in phase space. Simultaneously, we apply a standard procedure for obtaining an accurate power spectrum. To this end, we employ a fast-Fourier-transform algorithm to process a 4096-point time series of the velocity of the particle which was initially shaped by a cosine bell window of the Hanning type,[8] used to eliminate spurious frequency components associated with sharp edges in the time series. In Fig. 1(a), we show the power spectrum corresponding to the motion of a particle for the set of parameters $\alpha=16$, $\nu=85$, $\epsilon=0.09$, with initial values $x_0=0$, $v_0=5.8$. In this figure, major well-defined and separated peaks are clearly distinguished signifying an orderly motion of which the Poincaré section is shown in Fig. 2(a). Increasing ϵ up to the value $\epsilon=0.155$, keeping all the other parameters and initial values fixed, will not significantly change these pictures. For $\epsilon=0.156$, however, a chain of islands (of very small size) pattern in phase space appears [Fig. 2(b)], while the associated spectrum still remains characteristic of an orderly motion [Fig. 1(b)]. Increasing now ϵ to 0.158 results in a destruction of the chain of islands, the motion in phase space appearing to be chaotic, see Fig. 2(c), and in the corresponding spectrum a raised plateau is recognized with a diffuse structure of the peaks which is the Fourier characterization of stochastic motion [Fig. 1(c)]. To appreciate the changes in the spectrum, compare Figs. 1(c) and 1(a). As this characterization seems to be a very sensitive indicator of chaotic motion, we will use it in the following as the main visual criterion for detecting stochasticity.

According to the conventional picture of the onset of stochasticity, once the motion becomes unstable, any increase of the perturbation would only make the motion more chaotically unstable. Unexpectedly, it is found that when increasing ϵ to 0.18, the motion becomes stabilized, the spectrum recovering a nonchaotic pattern characterized by sharply distinguished nondiffuse peaks, see Fig. 1(d), and in the corresponding Poincaré section [Fig. 2(d)], a chain of islands [of much larger size than in Fig. 2(b)] pattern appears in phase space characterizing again nonchaotic motion. Increasing furthermore ϵ to 0.23 results in even a stronger stabilization effect, compare the spectra in Figs. 1(e) and 1(d); the Poincaré section corresponding to this value of the parameter is quite similar to the one given in Fig. 2(b). The further evolution of the system with the increase of the perturbation in its course for reaching final stochasticity might follow different routes. However, this study will not be undertaken in this work. In order to get an insight into this transitory phenomenon it is instructive to analyze in more detail the successive spectra associated with the different values of the perturbation. It is convenient to start this analysis by inspecting the simplest of the spectra given in Fig. 1, namely, Fig. 1(a). In this frame one clearly sees a most prominent peak that is associated with the free oscillation at frequency $\omega_0=5.59$ corresponding to the unperturbed motion of the particle, shifted, however, somewhat from this value due to the finiteness of the perturbation. Recognized in this figure is another major independent peak to the left of the "ω_0" peak at a frequency $\omega_1=4.358$.

Now, due to the nonlinearity of the system, all the ma-

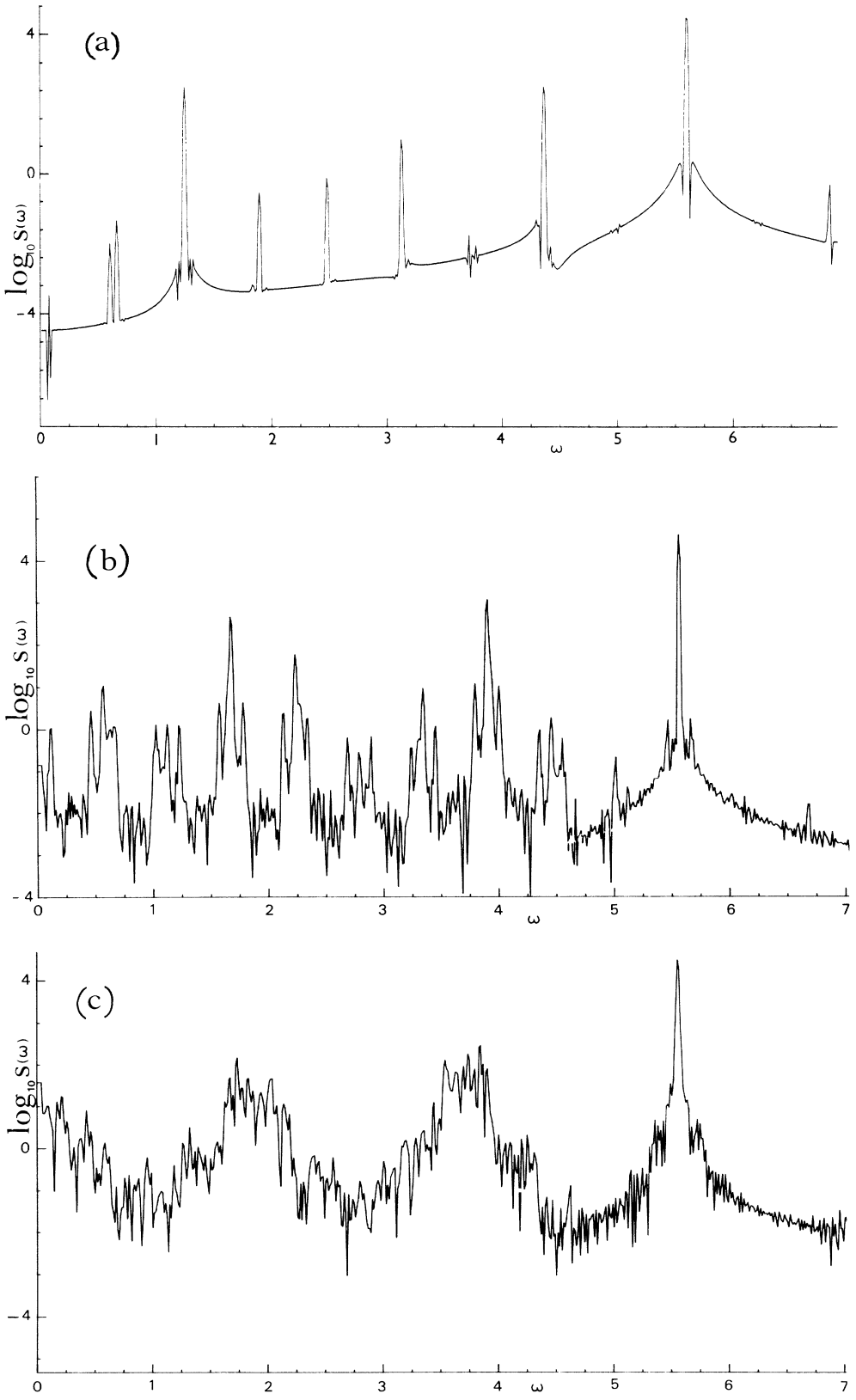

FIG. 1. (a) Power spectrum $S(\omega)$ of the solution $v(t)$ of Eq. (1), using a $\log_{10}$ scale, as a function of the angular frequency ω with initial conditions $x_0=0$, $v_0=5.8$, and parameters, $\alpha=16$, $\nu=85$, $\epsilon=0.09$. (b) Power spectrum for $\epsilon=0.156$. Initial conditions, other parameters, and equation of motion as in (a). (c) Power spectrum for $\epsilon=0.158$. Initial conditions, other parameters, and equation of motion as in (a). (d) Power spectrum for $\epsilon=0.18$. Initial conditions, other parameters, and equation of motion as in (a). (e) Power spectrum for $\epsilon=0.23$. Initial conditions, other parameters, and equation of motion as in (a).

jor other spectral lines appearing in the figure can be attributed to a linear combination of these two independent frequencies ω_0 and ω_1, in the form $\omega_i = m\omega_0 + n\omega_1$, where m and n take appropriate positive or negative integer values. The most important line resulting from this combination is clearly distinguished at $\omega_2 = \omega_0 - \omega_1 = 1.232$. The free frequency ω_0 depends only slightly on ϵ, while ω_1 does depend on it rather significantly, as can be seen by comparing the positions of the ω_1 peaks in the two frames (a) and (b) of Fig. 1.

Consequently, it is sufficient at this stage to follow the shift in position of the ω_1 peak with the changes of the perturbation for acquiring a comprehensive understanding of the evolution of the power spectrum of the system. Hence, we draw in Fig. 3 the value of the frequency of this ω_1 peak as a function of ϵ. For values of the perturbation parameter up to $\epsilon = 0.158$, one observes a monotonic decrease of the frequency ω_1 with ϵ. For $\epsilon = 0.158$, as stated before, the system becomes chaotic, characterized by a broad diffuse structure of this peak. This chaotic state continues up to $\epsilon = 0.167$ and is indicated by the dotted line in the figure. At $\epsilon = 0.167$ suddenly the motion gets stabilized. The position of the peak, however, when changing ϵ further up to the values considered in the figure, is fixed, locked to a specific value, being rational to ω_0 as $\omega_1/\omega_0 = \frac{2}{3}$. These observations are not confined to this specific example, but seem to be of a more general nature and are valid for various other examples as well. Another example similar to the one shown in Fig. 3 is given in Fig. 4.

From these observations, one is inclined to conclude that the intermediate stochasticity is inherently associat-

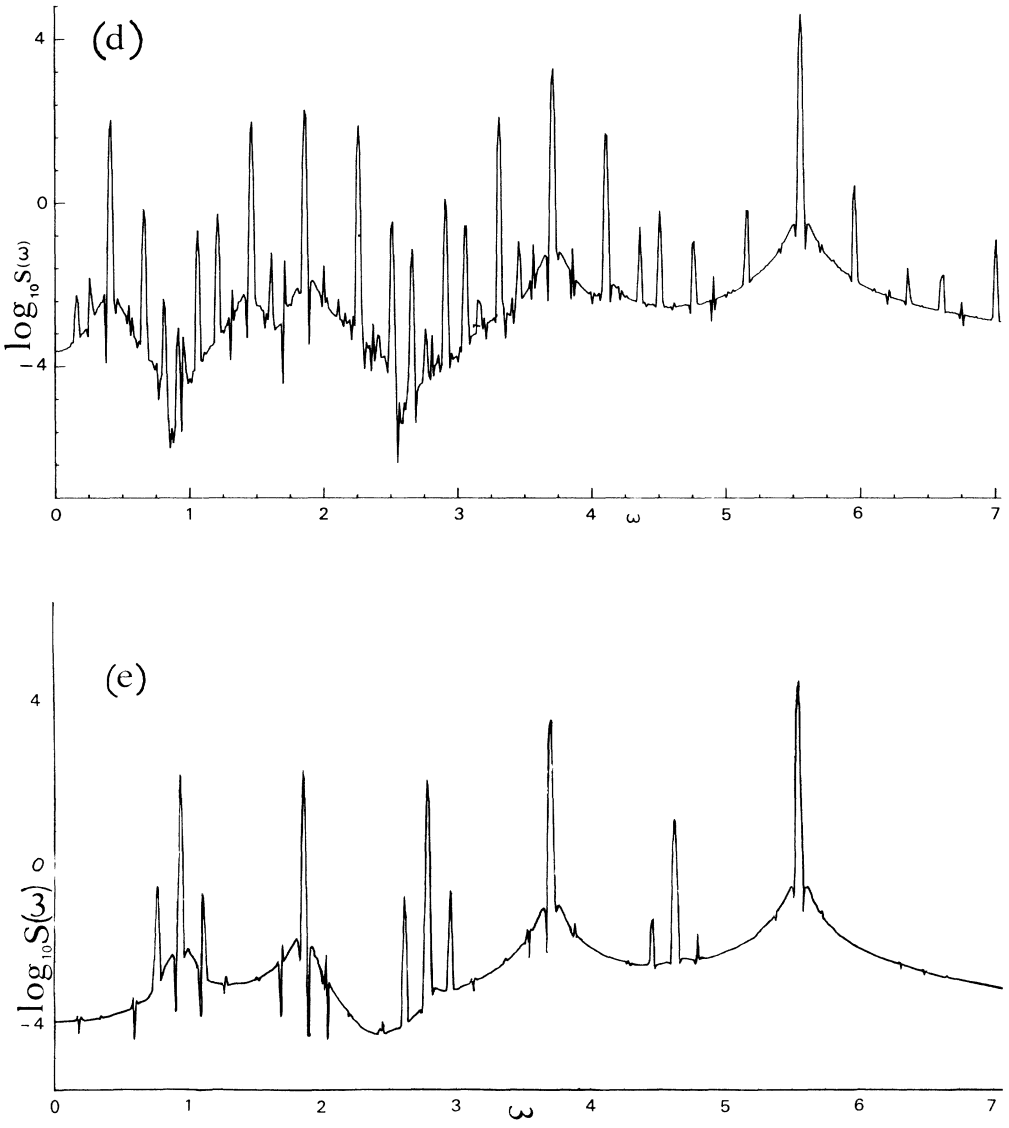

FIG. 1. (*Continued*).

ed with the threshold of the mode-locking phenomenon. This linkage will be elaborated theoretically in Sec. III.

III. MODE LOCKING AND SIDEBAND GENERATION IN THE TWO-WAVE SYSTEM

The mode-locking phenomenon is associated with effects due to nonlinear interaction taking place in the system, affecting the time dependency of the mode frequencies. A mode will be locked to a fixed frequency inherent to the system if its phase reaches a stable steady state. The analysis of this steady state involves generally the temporal development of the amplitude and the phase of the different modes. A very convenient formalism providing such a functional time dependency of these parameters is the theory of Krylov and Bogoliubov[5] (KB) as

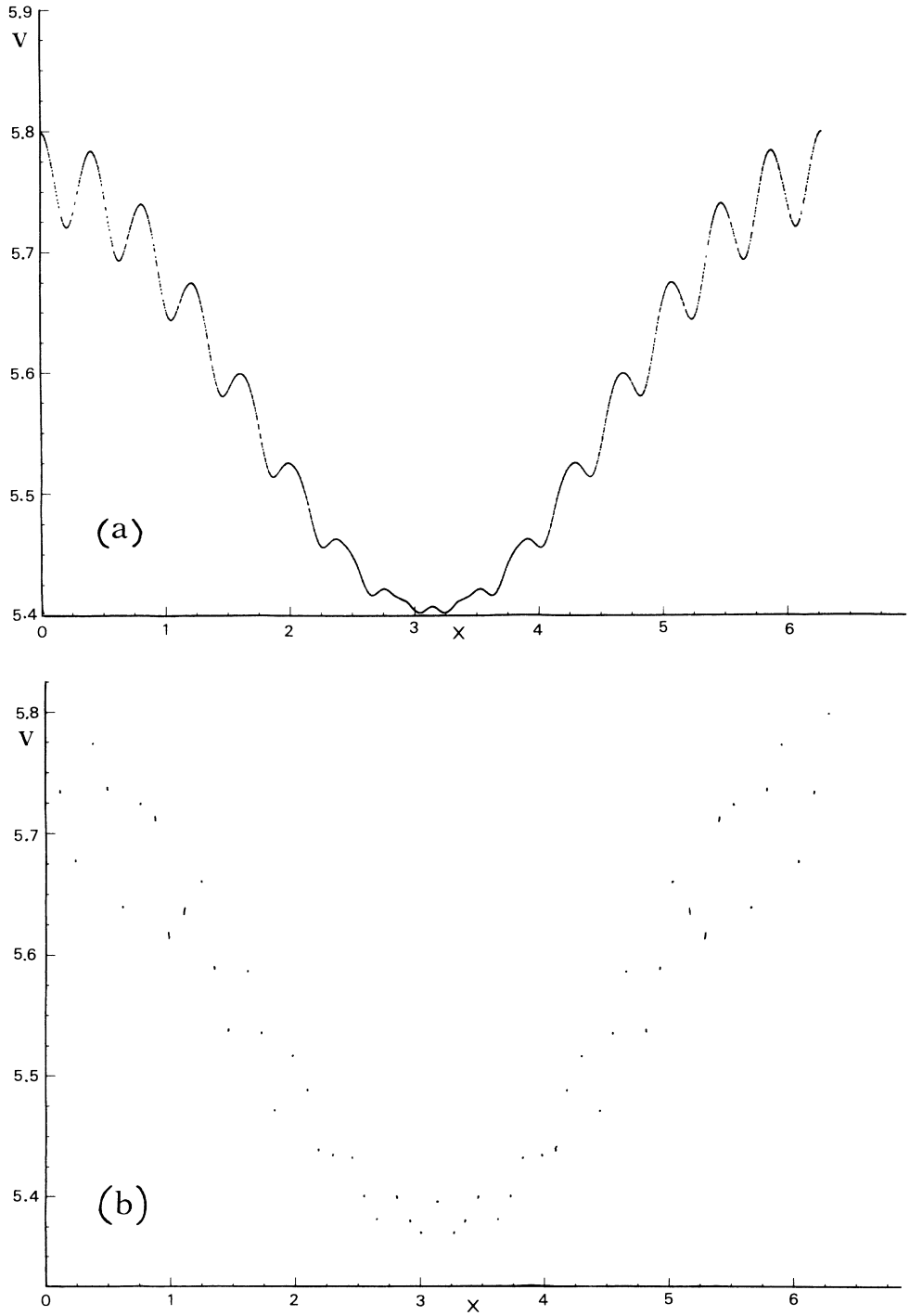

FIG. 2. (a) Particle trajectories in phase space (x,v) with x modulo 2π, viewed at successive times $t=2\pi,4\pi,\ldots,2N\pi$, with $N=4096$. The plot corresponds to the trajectories of one particle starting with initial conditions $x_0=0$, $v_0=5.8$, and parameters $\alpha=16$, $\nu=85$, $\epsilon=0.09$. (b) Same as (a) with $\epsilon=0.156$. (c) Same as (a) with $\epsilon=0.158$. (d) Same as (a) with $\epsilon=0.18$.

refined by Haag,[9] which employs the method of averaging in conjunction with the technique of variation of parameters. In terms of this formalism it is possible to express the temporal development of the amplitude and the phase of the modes in a set of two coupled first-order differential equations. Mode locking and synchronization phenomena are then, in general, searched for via this set of equations.

In order to facilitate the presentation of our analysis that utilizes the KB formalism, we will now briefly outline its basic features. After establishing in a general manner the form of the basic set of equations and the conditions for the existence of synchronous solutions, we will proceed to analyze the two-wave equation [Eq. (1)] and to express it into such a basic set form. The structure of the power spectrum of the two-wave system will

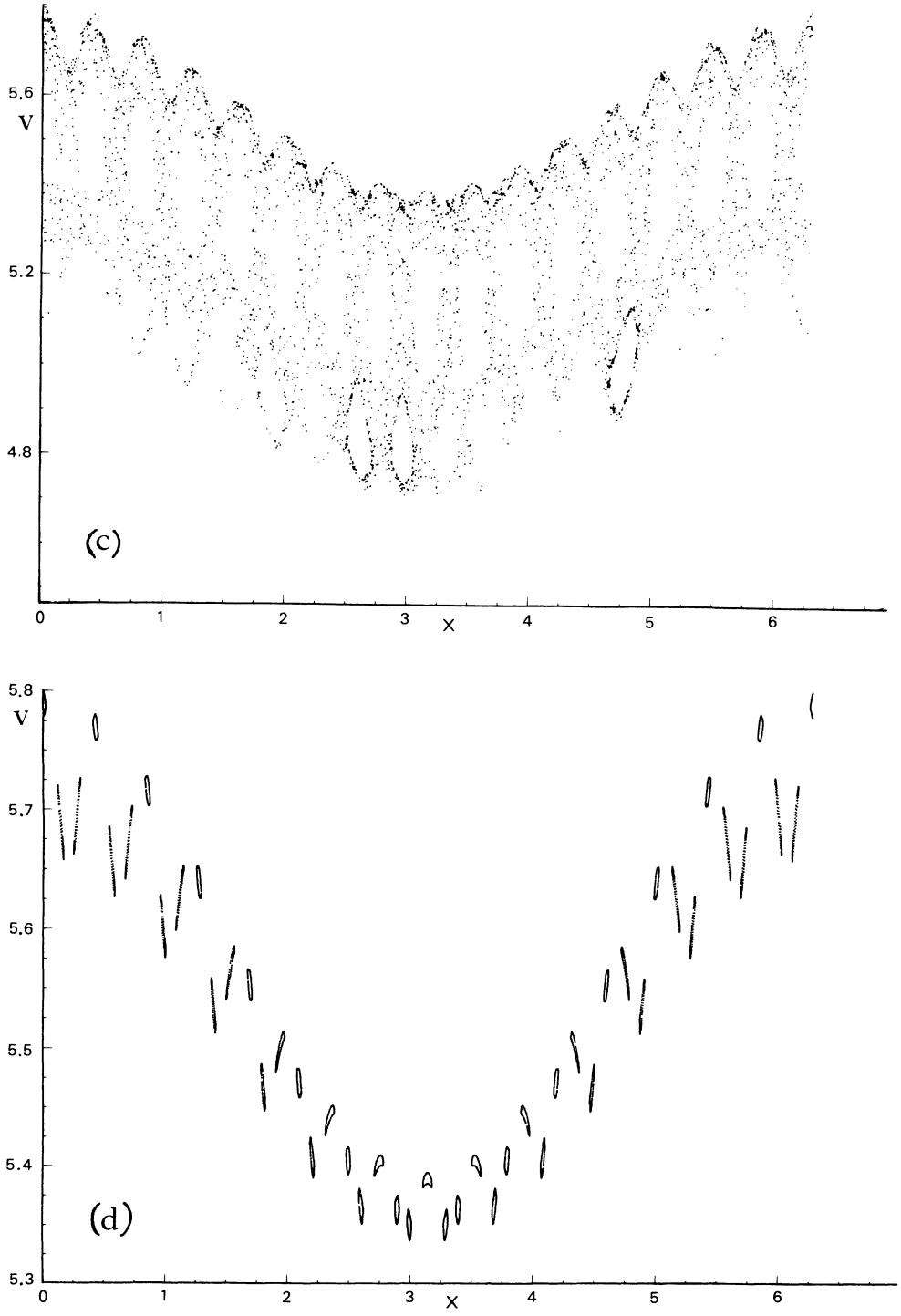

FIG. 2. (*Continued*).

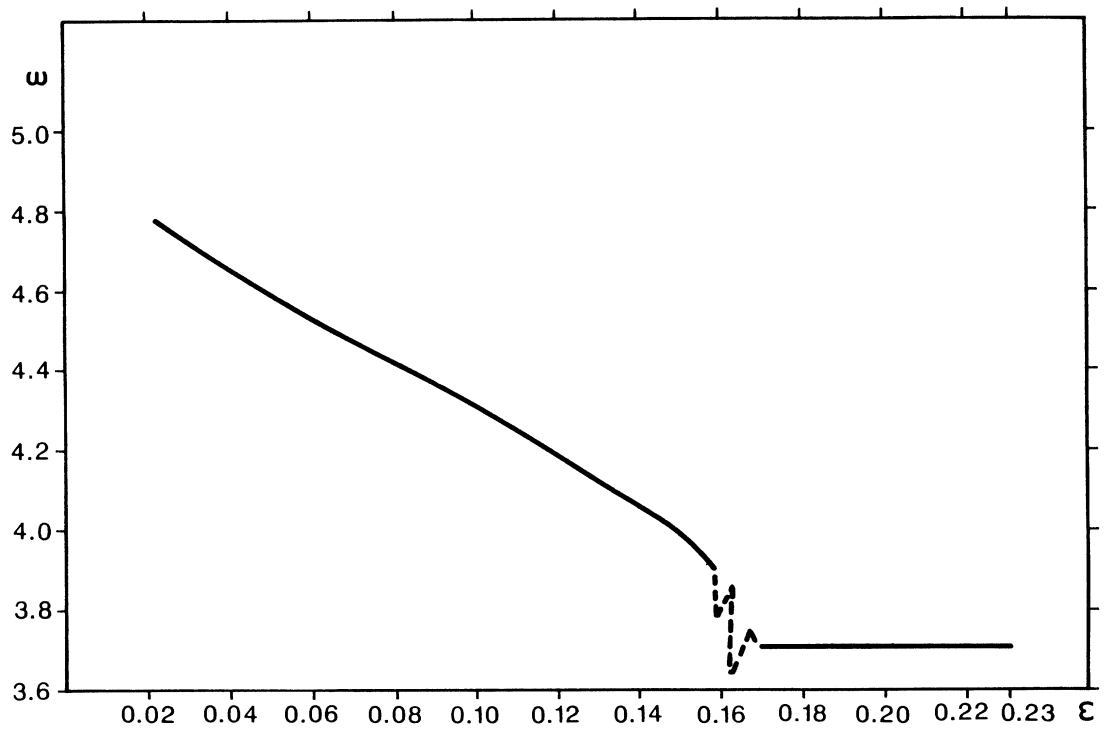

FIG. 3. The position in frequency of the "ω_1" peak defined in the text, as a function of the strength of the perturbation ϵ. The points on this graph are deduced from power spectra similar to those shown in Fig. 1 for initial values $x_0=0$, $v_0=5.8$, and parameters $\alpha=16$, $\nu=85$. The dotted points correspond to chaotic motion.

then be deduced from analyzing this set of equations.

The Krylov-Bogoliubov theory is a scheme for obtaining approximate solutions to certain types of second-order differential equations that include a small periodic perturbation term. The KB method, as proposed originally, was intended to provide approximate solutions to weakly nonlinear differential equations. However, generalizations of the method are possible.[10] Such generalizations enable one to obtain approximate solutions to some strongly nonlinear differential equations including

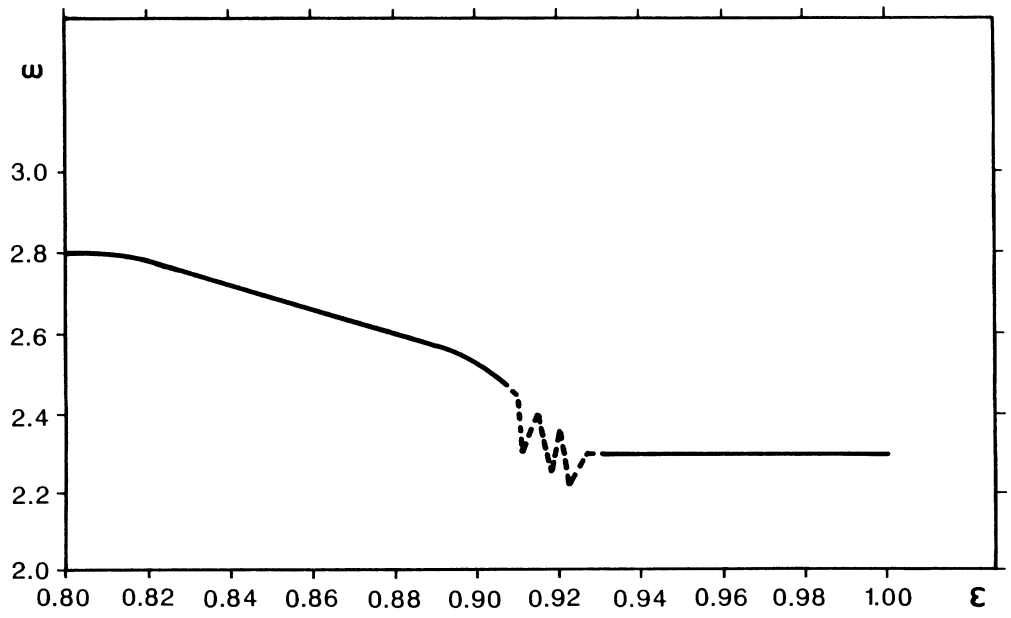

FIG. 4. Same as in Fig. 3, with initial values $x_0=4.71$, $v_0=4.5$, and parameters $\alpha=16$, $\nu=85$.

the basic equation of our problem, Eq. (1). The KB method starts from a generating solution which is the solution of the unperturbed equation of motion. This solution depends on two time-independent parameters, say, a and ϕ. It is assumed that the effect of the perturbation is to introduce a time dependency in the parameters a and ϕ without affecting the form of the expressions of both the unperturbed solution and its unperturbed derivative with respect to time. Using this assumption and expressing the perturbation term in a Fourier series in terms of the parameters a and ϕ, one arrives at a set of two first-order differential equations for a and ϕ. This set is the basic set of equations of the analysis. If the conditions of the problem under consideration are such that the nonderivative (with respect to time) terms appearing in the equations are of the same order of magnitude of the small parameter, say ϵ, characterizing the perturbation, it is then possible to write the basic set in the form

$$\frac{da}{dt}=\epsilon g(a,\phi,t) , \tag{2}$$

$$\frac{d\phi}{dt}=\epsilon h(a,\phi,t) , \tag{3}$$

where g and h are periodic functions in time with period T. Following Haag,[11] one introduces a set of associated functions A and Φ defined as

$$A(a,\phi)=\frac{1}{T}\int_0^T g(a,\phi,t)dt , \tag{4}$$

$$\Phi(a,\phi)=\frac{1}{T}\int_0^T h(a,\phi,t)dt , \tag{5}$$

where the variables a and ϕ under the integral sign are considered to be independent of time. It was shown by Haag[9] that for the same initial conditions $a(t=0)$ and $\phi(t=0)$ the solutions of the set of equations

$$\frac{da}{dt}=\epsilon A(a,\phi) , \tag{6}$$

$$\frac{d\phi}{dt}=\epsilon\Phi(a,\phi) \tag{7}$$

differ from those of Eqs. (2) and (3) at most by terms of order ϵ. This set of autonomous equations [Eqs. (6) and (7)] allows for the analysis of the steady-state solutions in the plane (a,ϕ) for the different modes of oscillation of the system. Haag's synchronization theory then asserts that the solutions for which the frequency of the mode under consideration is locked to the external perturbation frequency are those corresponding to the singular points of Eqs. (6) and (7), namely, the points in the plane (a,ϕ) for which $da/dt=d\phi/dt=0$. These solutions are referred to as synchronous solutions. Since $\epsilon\neq 0$, mode locking is associated with the simultaneous vanishing of the functions $A(a,\phi)$ and $\Phi(a,\phi)$.

As here we will be mainly interested in the behavior of the solutions of the equation of motion, Eq. (1), just outside the locking region, the synchronization process itself will not be of major interest to us in this work and therefore it will not be elaborated upon further. Motivated by the numerical results, we would like to investigate the dependency of power spectra on the strength of the perturbation. Thus, we will consider especially the dependency of the frequency $d\phi/dt$ (in our notation) on this parameter. We will try therefore to analyze the equation of motion, Eq. (1), bringing it to the form of the basic set of equations, Eqs. (2) and (3), the second of which is in a form which might be useful to our analysis. To this end we write Eq. (1) in the form of a set of two first-order equations in the variables x and v:

$$\frac{dx}{dt}=v , \tag{8}$$

$$\frac{dv}{dt}=-\sin(x)-\epsilon F(x,t) , \tag{9}$$

where

$$F(x,t)=\sin(\alpha x-\nu t) . \tag{10}$$

The Hamiltonian corresponding to the unperturbed motion reads

$$H_0=\frac{v^2}{2}-\cos x , \tag{11}$$

and is an exact integral of this motion. It is well known that for both cases of librational or rotational motions, corresponding, respectively, to $H_0<1$ or $H_0>1$, the motion is periodic. In order to exhibit the periodicity of this motion, we introduce an angle variable θ through the usual relation

$$\frac{d\theta}{dt}=\omega_0(H_0) , \tag{12}$$

where ω_0 is the frequency of the free oscillatory motion. From the constancy of H_0 and therefore of ω_0, one notes that H_0 and θ may serve as an alternative set of two independent entities. In terms of this Hamiltonian, Eqs. (8) and (9) of the unperturbed motion will read

$$\omega_0(H_0)\frac{dx}{d\theta}=v=\frac{\partial H_0}{\partial v} , \tag{13}$$

$$\omega_0(H_0)\frac{dv}{d\theta}=-\sin(x)=-\frac{\partial H_0}{\partial x} . \tag{14}$$

The variables x and v can now be expressed in terms of H_0 and θ or more conveniently[12] as functions of a and θ where $a^2=(1+H_0)/2$. When considering the equation of motion including the perturbation term, the variable a will now acquire a time dependency. In analogy with the Krylov-Bogoliubov approach for weakly nonlinear systems, we assume that the relations between x and v as given by Eqs. (13) and (14) are still valid when the perturbation is included. This method has been generalized by Cap[10] and utilized by us[7] for strongly nonlinear unperturbed equations, allowing for nonharmonic periodic solutions (in general expressed in terms of elliptic functions). Expressing then the total derivative of x and v with respect to time through the variables a and θ, the set of equations [(8) and (9)] reads

$$\frac{\partial x}{\partial\theta}\frac{d\theta}{dt}+\frac{\partial x}{\partial a}\frac{da}{dt}=\omega_0\frac{\partial x}{\partial\theta}\ , \tag{15}$$

$$\frac{\partial v}{\partial\theta}\frac{d\theta}{dt}+\frac{\partial v}{\partial a}\frac{da}{dt}=+\omega_0\frac{\partial v}{\partial\theta}-\epsilon F(x,t)\ . \tag{16}$$

Multiplying Eq. (15) by $-(\partial v/\partial\theta)$ and Eq. (16) by $\partial x/\partial\theta$ (assuming $\partial x/\partial\theta\neq 0$) and adding, one obtains

$$\frac{da}{dt}\left[\frac{\partial x}{\partial\theta}\frac{\partial v}{\partial a}-\frac{\partial x}{\partial a}\frac{\partial v}{\partial\theta}\right]=-\epsilon F(x,t)\frac{\partial x}{\partial\theta}\ . \tag{17}$$

Now multiplying Eq. (15) by $\partial v/\partial a$ and Eq. (16) by $-(\partial x/\partial a)$ and adding, we get

$$\left[\frac{d\theta}{dt}-\omega_0\right]\left[\frac{\partial x}{\partial\theta}\frac{\partial v}{\partial a}-\frac{\partial x}{\partial a}\frac{\partial v}{\partial\theta}\right]=\epsilon F(x,t)\frac{\partial x}{\partial a}\ . \tag{18}$$

Let us note that the Jacobian of the transformation $(\partial x/\partial\theta)(\partial v/\partial a)-(\partial x/\partial a)(\partial v/\partial\theta)$ has to be evaluated using the expressions of the dynamical variables x and v corresponding to the solution of the unperturbed motion and it is found to be explicitly $4a/\omega_0$, where use has been made of the relation $(1/\omega_0)(dH_0/da)=4a/\omega_0$; thus finally we find

$$\frac{da}{dt}=-\epsilon\frac{\omega_0}{4a}F(x,t)\frac{\partial x}{\partial\theta}\ , \tag{19}$$

$$\frac{d\theta}{dt}-\omega_0=+\epsilon\frac{\omega_0}{4a}F(x,t)\frac{\partial x}{\partial a}\ . \tag{20}$$

This last system [Eqs. (19) and (20)] is fully equivalent to the system of equations [(25) and (26)] derived in Ref. 7. For completing the change of variables in the equation of motion we have thus to evaluate the terms $F(x,t)(\partial x/\partial\theta)$ and $F(x,t)(\partial x/\partial a)$ as functions of a, θ, and t. To this end, we first introduce the function

$$G(a,\theta,t)=-\frac{1}{\alpha}\cos[\alpha x(a,\theta)-\nu t]$$

and express these terms as $(\partial G/\partial\theta)(a,\theta,t)$ and $(\partial G/\partial a)(a,\theta,t)$, respectively. Then, as in the standard procedure of the KB theory, we express $\cos[\alpha x(a,\theta)-\nu t]$ and $\sin[\alpha x(a,\theta)-\nu t]$ in a Fourier expansion. Hence, considering the motion of the particle far away from the separatrix corresponding to values of $a\gg 1$ in accordance with the numerical study, we express the solution of the unperturbed motion as[12]

$$x(a,\theta)=2\,\mathrm{am}[\beta(a,\theta),a^{-1}]\ , \tag{21}$$

$$v(a,\theta)=\pm 2a\,\mathrm{dn}[\beta(a,\theta),a^{-1}]\ , \tag{22}$$

where

$$\beta(a,\theta)=\frac{a\theta}{\omega_0(a)}=a(t-t_0)\ , \tag{23}$$

where t_0 is the initial time, the frequency is

$$\omega_0(a)=\frac{\pi a}{K(a^{-1})}\ , \tag{24}$$

$K(a^{-1})$ (Ref. 13) stands for the complete elliptic integral of first kind, and am and dn are the standard Jacobi elliptic functions. Utilizing the solutions $x(a,\theta)$ as given by Eq. (21) with $a\gg 1$, an approximate expression for $\cos[\alpha x(a,\theta)]$ and $\sin[\alpha x(a,\theta)]$ can be readily obtained to read

$$\begin{aligned}\sin[\alpha x(a,\theta)]&\cong\sum_{m=-\infty}^{m=+\infty}J_m[2\alpha u(a)]\sin(\alpha+m)\theta\ ,\\ \cos[\alpha x(a,\theta)]&\cong\sum_{m=-\infty}^{m=+\infty}J_m[2\alpha u(a)]\cos(\alpha+m)\theta\ ,\end{aligned} \tag{25}$$

with

$$u(a)=\frac{2q(a)}{1+q^2(a)}\ ,$$

where

$$q(a)=\exp-[\pi K^*(a^{-1})/K(a^{-1})]$$

is Jacobi's nome, the associated complete elliptic integral of the first kind $K^*(a^{-1})$ being equal to $K(1-a^{-2})$, and J_m are Bessel functions of order m. In deriving this expression, use has been made of the following approximate expansion for the function am:

$$\begin{aligned}\mathrm{am}[\beta(a,\theta),a^{-1}]\cong&\,\pi\beta(a,\theta)/2K(a^{-1})\\&+u(a)\sin[\pi\beta(a,\theta)/K(a^{-1})]\ .\end{aligned} \tag{26}$$

In terms of this Fourier expansion, using the function G introduced previously, Eqs. (19) and (20) will now read

$$\frac{da}{dt}=-\frac{\epsilon\omega_0(a)}{4a\alpha}\left[\cos(\nu t)\sum_{m=-\infty}^{m=+\infty}(\alpha+m)J_m(2\alpha u)\sin(\alpha+m)\theta-\sin(\nu t)\sum_{m=-\infty}^{m=+\infty}(\alpha+m)J_m(2\alpha u)\cos(\alpha+m)\theta\right]\ , \tag{27}$$

$$\frac{d\theta}{dt}-\omega_0(a)=-\frac{\epsilon\omega_0(a)}{2a}\frac{du}{da}\left[\cos(\nu t)\sum_{m=-\infty}^{m=+\infty}J'_m(2\alpha u)\cos(\alpha+m)\theta+\sin(\nu t)\sum_{m=-\infty}^{m=+\infty}J'_m(2\alpha u)\sin(\alpha+m)\theta\right]\ . \tag{28}$$

When inspecting Eqs. (27) and (28), one notices that the frequency of a given mode and the frequency of the external imposed oscillation ν may combine into a phase expression that allows for the occurrence of a resonance phenomenon. Previous experience[14] in analyzing such resonances shows that the analysis is facilitated by the introduction of a new stroboscopic phase:

$$\phi=\frac{p}{q}\theta-\nu t\ , \tag{29}$$

p and q being integers, which is a measure of the deviation of the system from exact resonance. In terms of this variable

ϕ, the equations of motion will read

$$\frac{da}{dt}=-\frac{\epsilon\omega_0(a)}{4a\alpha}\sum_{m=-\infty}^{m=+\infty}(\alpha+m)J_m(2\alpha u)\sin\left[(\alpha+m)\phi\frac{q}{p}+\nu t\left[(\alpha+m)\frac{q}{p}-1\right]\right], \tag{30}$$

$$\frac{d\phi}{dt}=\frac{p}{q}\omega_0(a)-\nu-\frac{p}{q}\frac{\epsilon\omega_0(a)}{2a}\frac{du}{da}\left\{\sum_{m=-\infty}^{m=+\infty}J'_m(2\alpha u)\cos\left[(\alpha+m)\phi\frac{q}{p}+\nu t\left[(\alpha+m)\frac{q}{p}-1\right]\right]\right\}. \tag{31}$$

Considering now initial values of the equation of motion in the range of a given p/q resonance, the stroboscopic frequency $\Omega=[p/q\omega_0(a)-\nu]$ will be a small quantity of the same order as the perturbation term in the phase equation (31), namely, ϵ. In this case, the system of equations (30) and (31) can be written in the form of the basic set of equations [Eqs. (2) and (3)].

Considering α to be a rational number of the form $\alpha=r/s$, r and s being integers, we get for the phase terms of Eqs. (30) and (31) the expression

$$\xi_m(t)=\frac{(r+ms)q\phi(t)}{ps}+\frac{\nu t}{ps}[(r+ms)q-sp] .$$

Since r, s, m, p, and q are integers $(r+ms)q-sp$ will also be an integer. Let $I_{r,m,s,q,p}$ denote this integer. By inspecting the second term of $\xi_m,(\nu t/ps)I_{r,m,s,q,p}$, one notices that when the time has changed from t to $t+T$ with $T=2\pi(ps/\nu)$, the second term of ξ_m will change by an integer multiple of 2π. If, as is assumed in the KB theory, on this time scale the change in ϕ is negligibly small compared to changes in the other term of the phase ξ_m, then, to a good approximation each harmonic term in the sum in Eq. (30) will fulfill the relation

$$\sin[\xi_m(t+T)]=\sin[\xi_m(t)] .$$

One thus concludes that the functions $g(a,\phi,t)$ and $h(a,\phi,t)$ in Eqs. (2) and (3) can be considered to be periodic functions of time with period $T=2\pi(ps/\nu)$. Applying now the Haag theorem to Eqs. (32) and (33) we first evaluate the associated functions A and Φ:

$$\begin{aligned}A(a,\phi)&=-\frac{\omega_0(a)s}{4ar}\frac{1}{T}\int_0^T dt\sum_{m=-\infty}^{m=+\infty}\left[\frac{r}{s}+m\right]J_m\left[2\frac{r}{s}u\right]\sin\left\{\left[\frac{r}{s}+m\right]\phi\frac{q}{p}+\nu t\left[\left[\frac{r}{s}+m\right]\frac{q}{p}-1\right]\right\}\\&=-\frac{\omega_0(a)s}{4ar}\left[\frac{r}{s}+m\right]J_m\left[2\frac{r}{s}u\right]\sin\phi ,\end{aligned} \tag{32}$$

$$\begin{aligned}\Phi(a,\phi)&=\Omega/\epsilon-\frac{p}{q}\frac{\omega_0(a)}{2a}\frac{du}{da}\frac{1}{T}\int_0^T dt\left[\sum_{m=-\infty}^{m=+\infty}J'_m\left[2\frac{r}{s}u\right]\cos\left\{\left[\frac{r}{s}+m\right]\phi\frac{q}{p}+\nu t\left[\left[\frac{r}{s}+m\right]\frac{q}{p}-1\right]\right\}\right]\\&=\frac{\Omega}{\epsilon}-\frac{p}{q}\frac{\omega_0(a)}{2a}J'_m\left[2\frac{r}{s}u\right]\frac{du}{da}\cos\phi ,\end{aligned} \tag{33}$$

where m is an integer having a value for which the condition $(r/s+m)(q/p)-1=0$ is fulfilled. Thus, to a good approximation one can write Eqs. (32) and (33) in the form

$$\frac{da}{dt}=-\frac{\epsilon\omega_0(a)}{4a\alpha}(\alpha+m)J_m(2\alpha u)\sin\phi , \tag{34}$$

$$\frac{d\phi}{dt}=\Omega-\epsilon\frac{p}{q}\frac{\omega_0(a)}{2a}\frac{du}{da}J'_m(2\alpha u)\cos\phi , \tag{35}$$

where we have denoted $\alpha=r/s$. One should note that choosing α to be a rational number of the form $\alpha=r/s$, as we did here, is not a very restrictive choice, since any nonrational α could be approximated rather closely by a rational number. Thus the analysis is approximately valid for real α as well.

From the numerical analysis, one realizes that the physical process taking place in the frequency region just in the vicinity of locking is determinant in originating the intermediate stochasticity. In order to study the behavior of the system in this region we rewrite Eq. (35) in the form

$$\frac{d\phi}{dt}=\Omega(1-\lambda\cos\phi) , \tag{36}$$

where

$$\lambda=\epsilon\frac{p}{q}\frac{\omega_0(a)}{2a}J'_m(2\alpha u)\frac{du}{da}\Big/\Omega . \tag{37}$$

Equation (37) has been extensively studied in the search for locking in engineering electrical problems; an early example is given in Ref. 15. Assuming, as is usually done,[15] that the entities Ω and λ are approximately independent of time having the free running oscillation values, we can solve this equation analytically. Considering the region just outside the locking range which corresponds to values of λ just less than 1, we proceed to integrate Eq. (36) in the form

$$\int \frac{d\phi}{1-\lambda\cos\phi} = \Omega t + \phi_0 , \tag{38}$$

where ϕ_0 is an initial phase which can be equal to zero without loss of generality. For $\lambda < 1$, the solution for ϕ can be expressed as[16]

$$\phi = 2\arctan\left[\left(\frac{1-\lambda}{1+\lambda}\right)^{1/2}\tan(\psi/2)\right] , \tag{39}$$

where

$$\psi = \Omega t(1-\lambda^2)^{1/2} . \tag{40}$$

One should notice that as λ is close to 1, in this region, the phase ψ might be very small. The important physical consequences of this fact will now be elaborated upon. As readily seen from expression (39), the phase ϕ is a periodic function of time. This allows for an attempt at a Fourier analysis of its time dependency. To this end, we first consider the Fourier decomposition of $\cos\phi$ and $\sin\phi$.

From Eq. (39),

$$\tan(\phi/2) = \left(\frac{1-\lambda}{1+\lambda}\right)^{1/2}\tan(\psi/2) ,$$

since

$$\cos\phi = \frac{1-\tan^2(\phi/2)}{1+\tan^2(\phi/2)} ,$$

one obtains

$$1-\lambda\cos\phi = \frac{1-\lambda^2}{1+\lambda\cos\psi} . \tag{41}$$

In order to facilitate the use of the standard Fourier series tables[16] for such expressions, it is convenient to define the auxiliary parameter μ as

$$\mu = \frac{-1+(1-\lambda^2)^{1/2}}{\lambda} . \tag{42}$$

In terms of this parameter, we write Eq. (41) as

$$1-\lambda\cos\phi = \left(\frac{1-\mu^2}{1+\mu^2}\right)\left(\frac{1-\mu^2}{1-2\mu\cos\psi+\mu^2}\right) . \tag{43}$$

The right-hand side of this last equation is immediately recognized as the Poisson kernel for which the Fourier trigonometric series is well known and given by

$$\frac{1-\mu^2}{1-2\mu\cos\psi+\mu^2} = 1+2\sum_{k=1}^{k=\infty}\mu^k\cos(k\psi) . \tag{44}$$

Thus,

$$\cos\phi = -\mu+\frac{1-\mu^2}{\mu}\sum_{k=1}^{k=\infty}\mu^k\cos(k\psi) . \tag{45}$$

Next, expressing $\sin\phi$ in terms of ψ as

$$\sin\phi = (1-\lambda^2)^{1/2}\sin\psi/(1+\lambda\cos\psi) ,$$

one obtains by following the same procedure[16]

$$\sin\phi = \frac{1-\mu^2}{\mu}\sum_{k=1}^{k=\infty}\mu^k\sin k\psi . \tag{46}$$

Now, the Fourier decomposition of the phase ϕ itself is readily obtained by integrating Eq. (36) with respect to time, utilizing the Fourier series of the expression $(1-\lambda\cos\phi)$ as given by Eq. (43). One finds

$$\phi = \psi+2\sum_{k=1}^{k=\infty}\frac{\mu^k}{k}\sin(k\psi) . \tag{47}$$

As was stated in Ref. 7, the equation of motion, Eq. (1), can be conveniently viewed as an equation of motion for a nonlinear pendulum driven by oscillatory force terms. The pendulum responds to the excitation of these driving terms in an oscillatory motion characterized by frequencies which are not far from the frequency of the driving terms themselves. The larger a driving term is, the larger will be its corresponding components in the power spectrum. Since the dominant terms in the perturbation are those associated with resonance effects, it is sufficient to consider these terms for studying the main features of the spectrum. The contribution to the perturbation, due to a dominant term associated with a resonance characterized by the integer m for which the relation $(\alpha+m)q=p$ holds is

$$\begin{aligned}\sin(\alpha x-\nu t)|_{\rm res} &\cong J_m(2\alpha u)\sin[(\alpha+m)\theta-\nu t] \\ &\cong J_m(2\alpha u)\sin\phi \\ &\cong J_m(2\alpha u)(1-\mu^2) \\ &\quad\times\sum_{k=1}^{k=\infty}\mu^{k-1}\sin[k\Omega(1-\lambda^2 t)^{1/2}] .\end{aligned} \tag{48}$$

As λ is proportional to ϵ, by changing the strength of the perturbation, the frequency $\Omega^*=\Omega(1-\lambda^2)^{1/2}$ might become very small, when λ is approaching 1. Thus, one can expect to observe in the power spectrum lines at low frequency having non-negligible amplitudes. The size of the amplitudes depend however on initial values and parameters of the system. Let us note that in the limit $\lambda\to 1$, which corresponds to the threshold of locking, $\Omega^*\to 0$ and no low-frequency spectral lines can be generated. To get further insight into the manifestation of these low-frequency modes, we consider explicitly the Fourier expansion of the velocity of the particle. Note that according to the basic assumption underlying the slow variation parameters method, the functional dependency of the velocity of the particle on the parameters of the system is still given by expression (22) corresponding to the unperturbed solution. Using the approximation of the standard Fourier expansion of the Jacobi's elliptic dn function[13] one gets

$$v = \pm\omega_0 a\left[1+\frac{u(a)}{2}\cos\theta\right] . \tag{49}$$

In order to facilitate the presentation we consider a simplified example where $p/q=1$ for which $\theta=\phi+\nu t$, corresponding to the case where the resonance frequency is the fundamental harmonic of the driving frequency ν. The case considered in the numerical study corresponds to a subharmonic resonance at a rational value of ν and will not be treated analytically here. For the case under

consideration

$$\cos\theta=\cos\phi\cos(\nu t)-\sin\phi\sin(\nu t)$$
$$=-\mu\cos(\nu t)+(1-\mu^2)\sum_{k=1}^{k=\infty}\mu^{k-1}\cos(k\psi+\nu t)\ . \tag{50}$$

Thus,

$$v=\pm\omega_0(a)\left[1-2u(a)\mu\cos(\nu t)+2u(a)\frac{1-\mu^2}{\mu}\sum_{k=1}^{k=\infty}\mu^k\cos(k\psi+\nu t)\right]\ . \tag{51}$$

In arriving at this expression, use has been made of expressions (45) and (46). From Eq. (51) one immediately realizes that the velocity power spectrum consists of lines corresponding to the resonance frequency (in this case ν) and sidebands separated from this frequency by values of $\Omega^*(d\psi/dt=\Omega^*)$. If λ is small, not close to the locking range, one expects to observe well-separated beat notes. However, when λ is close to 1, the separating frequency Ω^* becomes very small and a distorted beat note might appear. Due to the nonlinear coupling process taking place in the system, this low frequency and its harmonics are translated into the full spectrum, combining with all the existing peaks into a raised spectrum consisting of broad diffuse patterns. Such a structure has been indeed observed in the numerical study, signifying onset of stochasticity. Let us note that the amplitude of the low-frequency modes so generated, depending on the initial values and parameters affecting the Bessel coefficients, might be rather small and consequently the stochastization effect due to the coupling of these modes with the other peaks of the spectrum might be quite limited.

In conclusion, we have presented a numerical study of the two-wave system that reveals the phenomenon of intermediate stochasticity. This type of stochasticity is induced for a finite range of the strength of the perturbation and was found to be closely associated with the locking phenomenon of a specific mode to a fixed frequency inherent to the system. It was observed to occur for values of the perturbation just below the threshold for locking. The detection of this stochasticity was done via the Fourier spectral analysis of the velocity of the particle and the visual criterion for its onset was taken to be the observation of broad diffuse patterns including a low-frequency structure with considerable size. The theoretical analysis accompanying this numerical study consisted of employing the slow variation parameters technique in conjunction with an averaging procedure to establish a set of equations describing the evolution of these parameters. A slow phase variable associated with the occurrence of a resonance in the system was evaluated and its Fourier representation was presented. From this representation one concludes that for a perturbation close to the threshold of locking, a low frequency and its harmonics can be generated and translated into the complete spectrum, leading to stochasticity, in agreement with the observations of the numerical analysis. One should note that inherent to this picture is the possibility of the extinction of stochasticity when the threshold of locking is reached, consistent with intermediate stochasticity. Since the two-wave Hamiltonian system is a paradigm equation describing a variety of physical processes, one should expect this intermediate stochasticity phenomenon to be realized in systems relevant to these processes. The implications of this phenomenon to magnetic turbulence in toroidal devices are presently under investigation.

ACKNOWLEDGMENTS

One of us (Y.G.) would like to thank Dr. J. Tachon for his hospitality at the Centre d'Etudes Nucléaires de Cadarache during the winter of 1988-1989.

[1]A. N. Kolmogorov, Dokl. Akad. Nauk SSSR **98**, 527 (1954); V. I. Arnold, Sov. Math. Nauk **2**, 501 (1961); J. Moser, Nachr. Akad. Wiss. Göttingen, Math. Phys. **K1**, 1 (1962).

[2]B. V. Chirikov, Nuclear Physics Institute of the Siberian Section of the U.S.S.R. Academy of Sciences Report No. 267, 1969 [European Organization for Nuclear Research Translation No. 71-40, Geneva (1971)] (unpublished); Phys. Rep. **52**, 263 (1979).

[3]A. J. Lichtenberg and M. A. Lieberman, *Regular and Stochastic Motion* (Springer-Verlag, Berlin, 1983).

[4]Y. Gell and R. Nakach (unpublished).

[5]N. Krylov and N. N. Bogoliubov, *Introduction to Nonlinear Mechanics* (Princeton University Press, Princeton, NJ, 1947) (English translation by S. Lefshetz); N. N. Bogoliubov and Y. A. Mitropolskii, *Asymptotic Methods in the Theory of Nonlinear Oscillations* (Hindoustan, Delhi, 1961).

[6]B. Van der Pol, Philos. Mag. **43**, 700 (1922); **43**, 105 (1922); **43**, 142 (1922); **3**, 65 (1927).

[7]Y. Gell and R. Nakach, Phys. Rev. A **34**, 4276 (1986).

[8]P. I. Richards, IEEE Spectrum **4**, 83 (1967); G. D. Bergland, *ibid.* **42**, 42 (1969).

[9]J. Haag, Bull. Soc. Math. **25**, 257 (1947).

[10]F. F. Cap, Int. J. Nonlinear Mech. **9**, 441 (1974).

[11]J. Haag, *Oscillatory Motions* (Wadsworth, Belmont, CA 1955), translated by Reinhardt M. Rosenberg.

[12]A. B. Rechester and T. Stix, Phys. Rev. A **19**, 1656 (1979).

[13]P. F. Byrd and M. D. Friedman, *Handbook of Elliptic Integrals for Engineers and Scientists* (Springer-Verlag, Berlin, 1971).

[14]Y. Gell and R. Nakach, Phys. Rev. A **29**, 1520 (1984).

[15]H. L. Stover, Proceedings IEEE Lett. **25**, 310 (1966).

[16]I. S. Gradshteyn and I. M. Ryzhik, in *Table of Integrals, Series, and Products*, edited by Alan Jeffrey (Academic, New York, 1980).